Large quantum dots with small oscillator strength

S. Stobbe,[1,*] T. W. Schlereth,[2,3] S. Höfling,[2,3] A. Forchel,[2,3] J. M. Hvam,[1] and P. Lodahl[1,†]
[1]*DTU Fotonik, Department of Photonics Engineering, Technical University of Denmark, Ørsteds Plads 343, DK-2800 Kgs. Lyngby, Denmark*
[2]*Technische Physik, Universität Würzburg, Am Hubland, D-97074 Würzburg, Germany*
[3]*Wilhelm Conrad Röntgen-Center for Complex Material Systems (RCCM), Am Hubland, D-97074 Würzburg, Germany*
(Received 18 June 2010; revised manuscript received 15 October 2010; published 16 December 2010)

We have measured the oscillator strength and quantum efficiency of excitons confined in large InGaAs quantum dots by recording the spontaneous emission decay rate while systematically varying the distance between the quantum dots and a semiconductor-air interface. The size of the quantum dots is measured by in-plane transmission electron microscopy and we find average in-plane diameters of 40 nm. We have calculated the oscillator strength of excitons of that size assuming a quantum-dot confinement given by a parabolic in-plane potential and a hard-wall vertical potential and predict a very large oscillator strength due to Coulomb effects. This is in stark contrast to the measured oscillator strength, which turns out to be so small that it can be described by excitons in the strong confinement regime. We attribute these findings to exciton localization in local potential minima arising from alloy intermixing inside the quantum dots.

DOI: 10.1103/PhysRevB.82.233302 PACS number(s): 78.67.Hc, 42.50.Ct, 78.47.jd

Enhancement of light-matter interaction is important for improving existing optoelectronic devices such as light-emitting diodes and semiconductor lasers as well as for enabling envisioned devices for quantum information processing. The interaction between light and an emitter can be enhanced by modifying the environment surrounding the emitter, i.e., by increasing the optical field using nanophotonic cavities, which can be realized in many geometries such as microdiscs,[1] micropillars,[2,3] or photonic crystal cavities.[4,5] Cavity enhancement works by increasing the local density of optical states (LDOS), which describes the number of vacuum modes that an emitter can radiate into. Another approach to enhance the light-matter interaction is to modify the emitter, i.e., to tailor the matter part. The relevant figure of merit is the oscillator strength (OS), which is a dimensionless quantity defined as the ratio between the radiative decay rate of the emitter in a homogeneous medium and the emission rate of a classical harmonic oscillator.

Self-assembled quantum dots (QDs) are particularly interesting light-emitters because their OS is typically one order of magnitude larger than that of atoms.[6] Furthermore, as first pointed out by Hanamura,[7] the OS of excitons in a large QD is proportional to the volume of the QD: in this case Coulomb effects dominate the electron-hole confinement and the exciton acquires the sum of OSs of all lattice sites that it spans. This giant OS effect arises in the weak confinement regime, i.e., when the confinement is so weak that the energy level spacing is smaller than the Coulomb energy.

For small QDs the level spacing is much larger than the Coulomb energy and the exciton state can be described by a product of an electron state and a hole state, which are mutually independent. This is known as the strong confinement regime, which is the relevant regime for the majority of contemporary experiments. In the strong confinement approximation the OS is proportional to the square of the electron and hole envelope function overlap, which sets an upper limit to the achievable OS because the overlap cannot exceed unity.[8]

It was predicted by Andreani *et al.*[9] in 1999 that large QDs are essential to reach the strong coupling regime of light-matter interaction and indeed the vacuum Rabi splitting signature of strong coupling has been observed with large QDs.[1,3] Also, a very high OS of large GaAs QDs has been reported.[10] Here we report on direct measurements of the OS of large $In_{0.3}Ga_{0.7}As$ QDs and surprisingly observe no enhancement of the OS beyond the strong confinement limit.

The simplest way to measure the OS of a QD would be to extract it from a measurement of the radiative decay rate in a homogeneous medium. However, the radiative decay rate is not obtained directly by time-resolved spectroscopy, which extracts the total decay rate, i.e., the sum of radiative and nonradiative decay rates. The contribution from nonradiative decay processes was recently found to be significant for small QDs[8,11] and the nonradiative decay rate was not measured in any of the previous experimental studies on large QDs.

Here we use a recently developed experimental method[8,11] to accurately measure the radiative and nonradiative decay rates and thereby extract the OS and quantum efficiency (QE) of large InGaAs QDs. We find that the experimentally determined OS is below the upper limit of the strong confinement model and that the relatively fast decay rates originate from a QE of only 33%, i.e., the decay rate is dominated by nonradiative decay. Our results show that the effective confinement potential in QDs can be much smaller than the QD size, presumably due to local variations in strain and chemical composition of the QDs.

The maximum attainable OS of $In_xGa_{1-x}As$ QDs in the strong confinement model is given by[8,11]

$$f_{\mathrm{SC,max}}(\omega,x) = \frac{E_p(x)}{\hbar\omega} \tag{1}$$

with the Kane energy $E_p(x)=(28.8-7.3x)$ eV and $\hbar\omega$ is the exciton transition energy. In the weak confinement regime the decay rate can be calculated using Wigner-Weisskopf theory for excitons confined in a parabolic in-plane potential

perpendicular to the growth direction and a hard-wall potential along the growth direction. For the lowest-energy transition the OS is

$$f_{\mathrm{WC}}(\omega,x)=\frac{2E_p(x)}{\hbar\omega}\left(\frac{L}{a_0}\right)^2, \tag{2}$$

where L is the diameter of the center-of-mass wave function in the plane perpendicular to the growth direction,[12] which we define as four standard deviations of the Gaussian wave function and a_0 is the exciton Bohr radius, which is defined as $a_0=\frac{4\pi\hbar^2\epsilon_0\epsilon_r}{q^2m_0m}$, where ϵ_0 is the vacuum permittivity, ϵ_r is the relative dielectric constant of GaAs, q is the electron charge, m_0 is the electron rest mass, and $m=\frac{m_em_{\mathrm{hh}}}{m_e+m_{\mathrm{hh}}}$ is the reduced effective mass of the exciton composed of an electron with effective mass m_e and a heavy-hole with effective mass m_{hh}. It is important to note that the relation between the actual wave function size and L is a definition but we stress that by defining L as four standard deviations we are performing a conservative estimate in this context, i.e., the giant OS effect is underestimated.

The effective masses depend on the indium mole fraction of the QD and the heavy-hole effective mass is modified by strain. For $In_{0.3}Ga_{0.7}As$ we obtain $a_0=19.2$ nm using parameters from Ref. 8, where we are considering only the heavy-hole mass in the plane perpendicular to the growth direction.

The OS calculated in the weak confinement model is plotted in Fig. 1(A) along with the fundamental OS limit of the strong confinement model for various indium mole fractions. Thus, by comparing measured and calculated OS the proper confinement model can be identified and such an analysis is presented in the following.

Upon measurement of the radiative decay rate of a QD in a homogeneous medium $\Gamma_{\mathrm{rad}}^{\mathrm{hom}}(\omega)$ and the nonradiative decay rate $\Gamma_{\mathrm{nrad}}(\omega)$, the OS can be obtained directly from the equation

$$f(\omega)=\frac{6\pi m_0\epsilon_0c_0^3}{n(\omega)q^2\omega^2}\Gamma_{\mathrm{rad}}^{\mathrm{hom}}(\omega), \tag{3}$$

where c_0 is the speed of light in vacuum and $n(\omega)$ is the index of refraction of GaAs, which depends on ω as well as the temperature.[13] The QE is defined as

$$QE(\omega)=\frac{\Gamma_{\mathrm{rad}}^{\mathrm{hom}}(\omega)}{\Gamma_{\mathrm{rad}}^{\mathrm{hom}}(\omega)+\Gamma_{\mathrm{nrad}}(\omega)}. \tag{4}$$

The starting point of the experimental investigation was a semiconductor wafer grown by molecular beam epitaxy. First a 50 nm AlAs sacrificial layer for an optional epitaxial lift-off process was grown on a GaAs substrate. This was followed by 1038 nm of GaAs, a layer of large InGaAs QDs with a nominal indium content of 30%, and finally a 445 nm GaAs capping layer. The QDs were grown by submonolayer deposition as in Refs. 3 and 14 but differed by employing 30 growth interrupts of 0.5 s each. As we will show in the following, this difference in growth parameters resulted in significantly different QDs. In particular, the QDs studied here were smaller than those obtained without the growth interrupts yet larger than typical InAs QDs.[15,16] Second, the OS turned out to be comparable to or even smaller than that of typical InAs QDs.[8,11]

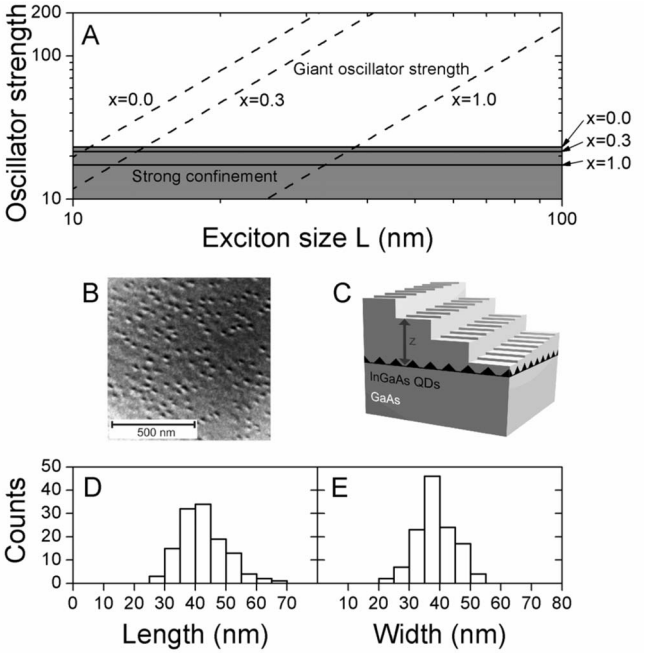

FIG. 1. (A) Calculated OS for $In_xGa_{1-x}As$ QDs with $x=0$, $x=0.3$, and $x=1$. In the weak confinement model (dashed curves) the OS increases quadratically with exciton size, which is known as the giant OS effect. In strong confinement there is an upper bound (solid curves) to the OS at $f=23.2$. The gray area indicates the regime of strong confinement for various mole fractions x. (B) In-plane transmission electron micrograph of the overgrown $In_{0.3}Ga_{0.7}As$ QDs. (C) Schematic illustration of the sample investigated. (D) Distribution of QD lengths along the major axis. (E) Distribution of QD widths along the minor axis. The average size along the major (minor) axis is found to be 42 nm (38 nm).

The QDs had a density of approximately 150 μm^{-2} and were slightly elliptically shaped with typical major and minor axis diameters of 42 nm and 38 nm, respectively, as determined from in-plane transmission electron microscopy on the overgrown sample,[17] cf. Figs. 1(B), 1(D), and 1(E). Thus, from Eq. (2) and cf. Fig. 1(A) we would expect $f \gtrsim 100$ for these QDs.

The capping layer was processed into 32 terraces, which measured 200×500 μm^2 thus constituting 32 different distances from the QD layer to the interface, as shown in Fig. 1(C). For each distance we have performed time-resolved measurements of QD ensembles at a temperature of 19 K and for one distance we performed time-resolved microphotoluminescence spectroscopy on single QDs at 10 K. All measurements were acquired using pulsed excitation from a Ti:sapphire laser at a wavelength of 860 nm, i.e., in the wetting layer of the QDs. The spectral resolution was 3.7 meV, i.e., we probed spectrally selected subensembles. Further details on the sample preparation, measurement setup, and theoretical approach can be found in Ref. 8. In the following we discuss the experimental results.

In Fig. 2(A) we show two characteristic decay curves for two different distances to the interface. The decays are markedly different due to the different values of the LDOS. We fit

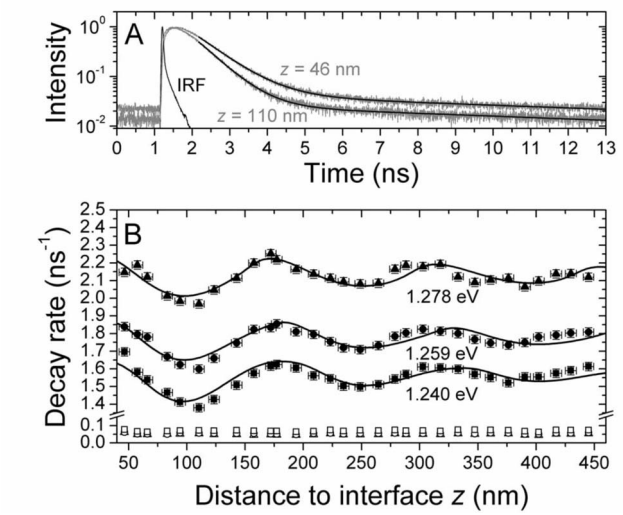

FIG. 2. (A) Characteristic decay curves (gray) of QDs obtained at two different distances to the interface at an emission energy of 1.240 eV with biexponential fits (black). The curve labeled IRF is the instrument response function. (B) Fast (closed symbols) and slow (open symbols) decay rates obtained from the biexponential fits for various distances to the interface at an emission energy of 1.240 eV (squares), 1.259 eV (circles), and 1.278 eV (triangles).

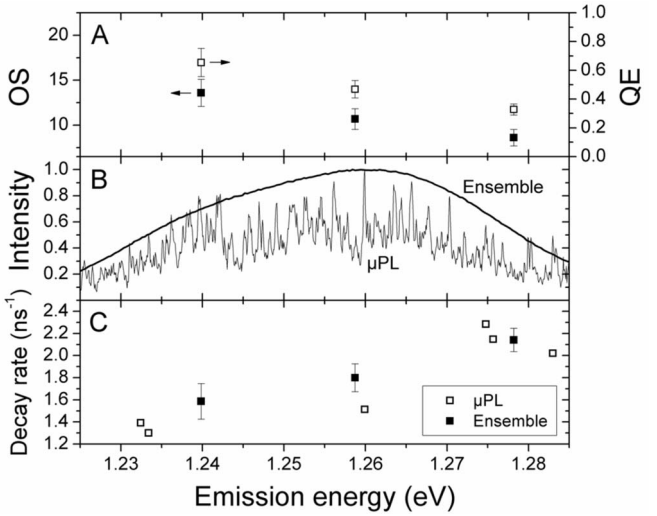

FIG. 3. (A) Oscillator strength (solid symbols, left axis) and QE (open symbols, right axis) for different emission energies obtained from the ensemble measurements. (B) Normalized photoluminescence spectrum obtained by ensemble and microphotoluminescence measurements at $z=445$ nm. (C) Total homogenous medium decay rate (solid symbols) extracted from the analysis of Fig. 2 compared to the microphotoluminescence measurements of the total decay rate at $z=445$ nm (open symbols).

the curves by biexponential decay functions convoluted with the instrument response function and find very good agreement. We have measured and fitted the decay curves for 32 distances to the interface and at three different emission energies of the QD ensemble. For the two distances closest to the interface ($z=12$ and 28 nm) we observe no photoluminescence, which presumably is due to tunneling of carriers to the surface followed by nonradiative recombination. The extracted fast and slow components for the remaining 30 distances are shown in Fig. 2(B). The slow decay rate is independent of distance to the interface, which shows that it is dominated by nonradiative decay.[18] In the remainder of this article we discuss only the fast decay rate, which exhibits a characteristic oscillatory behavior as a function of distance.

We have calculated the LDOS for a dipole source oriented parallel to the interface. The calculation is exact and takes all layers above and below the QDs into account. We have fitted the decay rate to the LDOS as a function of distance to the interface and we find very good agreement as is evident from the fits shown in Fig. 2(B).

The fit to the LDOS for each emission energy has two free parameters: the radiative decay rate and the nonradiative decay rate in a homogeneous medium. From this we obtain readily the OS and QE as well as their experimental uncertainties. The result of this analysis is shown in Fig. 3(A). We observe a frequency dependence, which is similar to that observed for small QDs,[8] i.e., both the OS and the QE decrease with increasing energy. However, in the present case the nonradiative decay rate is much larger leading to QEs between $(65\pm10)\%$ and $(33\pm4)\%$. These results show that the OS is not particularly large for these large QDs. In fact the OS is smaller than the limit imposed by the strong confinement model, cf. Fig. 1(A). Thus, no giant OS effect is observed and the OS can be described fully within the strong confinement model. Interestingly, the OS varies between 13.6 ± 1.5 and 8.6 ± 0.9, which is comparable to or even below the values found for ordinary QDs.[11]

It could be conjectured that only a small fraction of the large QDs possess a large OS. If this fraction was significant, this would result in decay curves with fast features and deviations from the biexponential decay; neither of which was observed. There could also be a contribution from charged excitons but the analysis in Ref. 8 showed that the frequency-dependent decay dynamics of QD ensembles can be described well by considering only neutral excitons. However, a comparison to microphotoluminescence experiments is needed to ensure that the ensemble measurements reflect average QD properties. We performed such an experiment and measured the spectrum shown in Fig. 3(B), which has been obtained at an excitation power below saturation of the excitons and with a spectral resolution of 250 μeV. Single QD lines are observed but the density of lines in the spectrum is surprisingly high considering the diffraction-limited confocal experimental condition. The result of time-resolved measurements on a selection of the peaks is presented in Fig. 3(C). The decay rates agree very well with the total decay rates extracted from the ensemble measurements, which are also shown in Fig. 3(C). Due to the high spectral density of excitonic transitions we cannot rule out the influence of more than one exciton on the microphotoluminescence results and one of these could potentially have a large OS. Since the number of excitons contributing to the decay curves in the microphotoluminescence case would be very small that would surely lead to decay curves with fast features and deviations from biexponential decay. Also in this case such effects are not observed, which shows that even if several excitons do contribute to the measurements they have very

similar optical properties and in particular comparable OSs. Thus, although the statistics is limited, this indicates that our measurements on ensembles are representative of average single QD properties.

We stress that our results do not exclude the possibility that very few QDs in our sample could possess a large OS. Also, our results do not imply that the giant OS cannot exist in large QDs grown under different conditions. What we can simply conclude is that no indications of the giant OS effect are observed in any of our measurements. Our work emphasizes the importance of measuring the QE of solid-state emitters because the prevalent assumption $QE(\omega)=1$ is generally not valid. In the present case this erroneous assumption would lead to overestimates of the OS by up to a factor of 3.

Our results show that the effective size of the excitons is much smaller than the size of the QDs as it appears from transmission electron microscopy. This means that the confinement potential is significantly smaller than the QD size and we conjecture that the actual confinement potentials are defined by fluctuations in the local indium/gallium mole fraction. Such fluctuations have been observed in high-resolution transmission electron microscopy studies of small InAs QDs[15,16] and our results suggest that they may be crucial for the optical properties of large QDs. In this picture the excitons are confined in potential minima surrounded by barriers and other local potential minima. This could imply large nonradiative decay rates due to transfer to other local minima, which is exactly what we observe. Furthermore, transfer by, e.g., tunneling of carriers into the potential minimum responsible for recombination from other nonradiative minima could lead to filling effects in the decay curves, i.e., decay curves, which appear flat on the top due the re-excitation provided by the charge transfer, which is also a feature that is apparent in our measurements, cf. Fig. 2(A). We note that such decay curve shapes could also indicate saturation of the QDs but this is not the case here, since we apply an excitation power below saturation. Our hypothesis of several potential minima in the dots is supported by the high spectral density of microphotoluminescence lines but it is not clear whether tunneling or another mechanism is causing the carrier transfer. In an alternative picture, alloy fluctuations could lead to localization of excitons in a single minimum[19] but this model does not explain the fast nonradiative decay rate. Further investigations are needed to clarify the origin of the nonradiative recombination.

Finally, we note that similar deviations between the size of the device and the effective potentials have been reported for other mesoscopic electronic systems, such as GaN/AlN QDs,[19] interface fluctuation QDs in quantum wells,[10] unintentional QDs in high-mobility two-dimensional electron gases,[20] and carbon nanotubes, where the effective QD size is given by the distance between the electrical contacts rather than the length of the nanotubes.[21]

In conclusion we have measured the OS and QE of large InGaAs QDs. We find that the decay dynamics is dominated by nonradiative decay processes and that the OS is comparable to or even smaller than the values reported for small QDs. We conclude that the size of the actual confinement potential in these QDs is much smaller than the QD size obtained from transmission electron microscopy on the overgrown sample. Our results emphasize the importance of measuring the QE of QD emitters because the prevalent assumption of a QE of unity is generally not valid and can lead to wrong conclusions.

We would like to acknowledge P. T. Kristensen and J. E. Mortensen for valuable theoretical discussions, and Q. Wang for assistance with the microphotoluminescence measurements. We gratefully acknowledge the Danish Research Agency (Projects No. FNU 272-05-0083, No. FNU 272-06-0138, No. FTP 274-07-0459, and No. FTP 10-080853) and the European Commission (Project QPhoton) for financial support.

*ssto@fotonik.dtu.dk
†www.fotonik.dtu.dk/quantumphotonics

[1] E. Peter *et al.*, Phys. Rev. Lett. **95**, 067401 (2005).
[2] J. M. Gérard *et al.*, Phys. Rev. Lett. **81**, 1110 (1998).
[3] J. P. Reithmaier *et al.*, Nature (London) **432**, 197 (2004).
[4] T. Yoshie *et al.*, Nature (London) **432**, 200 (2004).
[5] A. Laucht *et al.*, New J. Phys. **11**, 023034 (2009).
[6] Z. Hens, Chem. Phys. Lett. **463**, 391 (2008).
[7] E. Hanamura, Phys. Rev. B **37**, 1273 (1988).
[8] S. Stobbe *et al.*, Phys. Rev. B **80**, 155307 (2009).
[9] L. C. Andreani *et al.*, Phys. Rev. B **60**, 13276 (1999).
[10] J. Hours *et al.*, Phys. Rev. B **71**, 161306 (2005).
[11] J. Johansen *et al.*, Phys. Rev. B **77**, 073303 (2008).
[12] M. Sugawara, Phys. Rev. B **51**, 10743 (1995).
[13] S. Gehrsitz *et al.*, J. Appl. Phys. **87**, 7825 (2000).
[14] A. Löffler *et al.*, J. Cryst. Growth **286**, 6 (2006).
[15] M. De Giorgi *et al.*, Phys. Status Solidi B **224**, 17 (2001).
[16] P. Wang *et al.*, Appl. Phys. Lett. **89**, 072111 (2006).
[17] P. Werner *et al.*, Cryst. Res. Technol. **35**, 759 (2000).
[18] J. Johansen *et al.*, Phys. Rev. B **81**, 081304(R) (2010).
[19] F. Rol *et al.*, Phys. Rev. B **75**, 125306 (2007).
[20] J. Ebbecke *et al.*, Phys. Rev. B **72**, 121311(R) (2005).
[21] S. Sapmaz *et al.*, Phys. Rev. B **71**, 153402 (2005).